Molecular Mechanism of VanHst, an α-Ketoacid Dehydrogenase Required for Glycopeptide Antibiotic Resistance from a Glycopeptide Producing Organism†

C. Gary Marshall, Michela Zolli, and Gerard D. Wright*

Antimicrobial Research Centre, Department of Biochemistry, McMaster University, 1200 Main Street West, Hamilton, ON, Canada, L8N 3Z5

Received December 2, 1998; Revised Manuscript Received April 22, 1999

ABSTRACT: The vancomycin resistance enzyme VanH is an α-ketoacid dehydrogenase that stereospecifically reduces pyruvate to D-lactate, which is required for the synthesis of the depsipeptide D-alanine-D-lactate. This compound then forms an integral part of the bacterial cell wall replacing the vancomycin target dipeptide D-alanine-D-alanine, thus the presence of VanH is essential for glycopeptide resistance. In this work, the VanH homologue from the glycopeptide antibiotic producing organism *Streptomyces toyocaensis* NRRL 15009, VanHst, has been overexpressed in *Escherichia coli* and purified, and its substrate specificity and mechanism were probed by steady-state kinetic methods and site-directed mutagenesis. The enzyme is highly efficient at pyruvate reduction with $k_{cat}/K_m = 1.3 \times 10^5$ M^{-1} s^{-1} and has a more restricted α-ketoacid substrate specificity than VanH from vancomycin resistant enterococci (VRE). Conversely, VanHst shows no preference between NADH and NADPH while VanH from VRE prefers NADPH. The kinetic mechanism for VanHst was determined using product and dead-end inhibitors to be ordered BiBi with NADH binding first followed by pyruvate and products leaving in the order D-lactate, NAD^+. Site-directed mutagenesis indicated that Arg237 plays a role in pyruvate binding and catalysis and that His298 is a candidate for an active-site proton donor. Glu266, which has been suggested to modulate the pK_a of the catalytic His in other D-lactate dehydrogenases, was found to fulfill a similar role in VanHst, lowering a pK_a value of k_{cat}/K_m nearly 2 units. These results now provide the framework for additional structure and inhibitor design work on the VanH family of antibiotic resistance enzymes.

Bacterial resistance to the glycopeptide antibiotics, which include the clinically important compounds vancomycin and teicoplanin, has had a profound effect on the current and future use of these drugs for the treatment of serious infections caused by Gram-positive bacteria. The major problem at this juncture is the rise of vancomycin resistant enterococci (VRE), which has emerged over the past decade as a serious source of hospital-acquired infection. High level glycopeptide resistance in VRE requires the biosynthesis of peptidoglycan terminating in D-alanine-D-lactate (D-Ala-D-Lac) rather than the virtually ubiquitous D-Ala-D-Ala (*1*, *2*). This inducible shift in peptidoglycan structure involves the expression of a unique D-Ala-D-Lac biosynthetic pathway which requires three novel enzymes: VanA/B, a D-Ala-D-Lac synthetase, VanX, a D-Ala-D-Ala specific hydrolase, and VanH, an α-ketoacid reductase which supplies sufficient levels of D-Lac.

This specialized D-Ala-D-Lac synthesis mechanism appears to originate in the bacteria which produce glycopeptide antibiotics where we have recently found a gene cluster consisting of *vanH*, *vanA*, and *vanX* homologues in the identical arrangement as the genes found on transposable elements in VRE (*3*). The VanA equivalents, DdlM from *Streptomyces toyocaensis* NRRL 15009 which produces the "aglyco"-glycopeptide A47934 and DdlN from *Amycolatopsis orientalis* C329.2 which produces vancomycin, have been characterized and shown to be bona fide D-Ala-D-Lac ligases with enzymatic properties which closely mirror the VanA and VanB ligases from VRE (*4*−*6*). The *S. toyocaensis* NRRL 15009 VanX homologue, VanXst, has recently been purified and characterized as well, and it has the expected D-Ala-D-Ala peptidase activity (*7*). Both the VanA and VanX homologues found in glycopeptide producing organisms have the predicted catalytic activities, but there are differences when compared to the enzymes from VRE. For example, VanXst has 10-fold higher k_{cat}/K_m for D-Ala-D-Ala than VanX from *Enterococcus faecium* (*7*), and DdlN from *A. orientalis* C329.2 shows a restricted substrate specificity in terms of the flexibility of the D-α-hydroxy acid tolerated in the C-terminal position compared to the VRE enzyme VanA (*6*).

In contrast to the VanA and VanX enzymes, there has been relatively little detailed work describing the α-ketoacid reductase VanH from any system. The VanH enzymes from VRE and antibiotic-producing bacteria show significant amino acid sequence homology to the D-lactate dehydrogenase (D-LDH) family of enzymes (*3*, *8*). A recent three-dimensional structure of the D-LDH from *Lactobacillus plantarum* (since renamed *Lactobacillus pentosus*) (*9*) provides a point of reference for mechanistic analysis not only for this particular enzyme but also for the VanH enzymes which share primary sequence homology and, presumably,

† This work was funded by the Natural Sciences and Engineering Research Council of Canada (NSERC), by a Medical Research Council of Canada Graduate (MRC) Studentship to C.G.M., and by an MRC Scholar Award to G.D.W.

* To whom correspondence should be addressed. Phone: (905) 525-9140 ext. 22943. Fax: (905) 522-9033. Email: wrightge@fhs.csu.mcmaster.ca.

10.1021/bi982843x CCC: $18.00
Published on Web 06/03/1999

structural similarity with D-LDH. In principle, a compound which inhibits any of the Van enzymes could find use as a potentiator of glycopeptides in the clinic where resistance is an issue. Inhibitor design requires a thorough understanding of enzyme mechanism and structure. We have initiated mechanistic work on the Van enzymes from glycopeptide antibiotic-producing bacteria as these enzymes provide not only an opportunity for study of important antibiotic resistance determinants but provide additional access to proteins which may be more amenable for structural analysis than the enzymes from VRE. We report herein the characterization of the mechanism of VanHst through steady state kinetics and site-directed mutagenesis. These studies now provide the appropriate background for future function and structure research within the VanH family of enzymes.

MATERIALS AND METHODS

Materials. NADH, NADPH, $NADP^+$, sodium pyruvate, lithium D-lactate, sodium oxamate, α-ketobutyrate, α-ketocaproate, α-ketoisocaproate, α-ketoisovalerate, and phenylpyruvate were purchased from Sigma. NAD^+ (free acid) was purchased from Boehringer Mannheim.

Overexpression of VanHst in Escherichia coli. The *vanHst* gene was amplified employing Vent polymerase using the genomic library clone pBlutoyddl3.0 as template (*3*). Reactions contained 100 ng of template, 10 mM KCl, 20 mM Tris-HCl, pH 8.8, 10 mM $(NH_4)_2SO_4$, 0.1% Triton X-100, 4 mM $MgSO_4$, 5.0% (v/v) DMSO, 0.4 mM dNTP's, 1 μM of each of 5′-GCTCTAGACATATGACCCACAGCGAGAAGG-3′ and 5′-TGACATAAGCTTAGTCTGG CCATGCTGATTCC-3′, and 2 units of Vent polymerase. Amplification reactions consisted of 25 cycles of 94, 50, and 72 °C for 1, 1.5, and 1.5 min, respectively. The approximately 1.0 kb product was digested with *Nde*I and *Hin*dIII, purified, and ligated to similarly treated pET22b (Novagen) by standard methods. A recombinant clone (pETVanHst) was identified and completely sequenced to ensure no mutations occurred during amplification. DNA sequencing was performed by Dr. Brian Allore using an ABI automated sequencer at the MOBIX central facility at McMaster University.

Purification of VanHst. E. coli BL21(DE3)/pETVanHst (1 L) was grown at 37 °C, 250 rpm, to mid-log phase in Luria Broth supplemented with ampicillin to 50 μg/mL. Protein expression was induced by the addition of isopropyl β-D-thiogalactopyranoside to 1 mM, and cells were harvested following additional growth for 3 h. Harvesting and washing yielded 2.5 g (wet weight) of cells which were suspended in 20 mL of lysis buffer containing 100 mM Hepes, pH 7.5, 300 mM NaCl, 1 mM EDTA, 1 mM dithiothreitol, and 1 mM phenylmethanesulfonyl fluoride, and passed twice through a French pressure cell at 20 000 psi. The extract was clarified by centrifugation at 10000*g*, and soluble proteins were subsequently fractionated by the addition of ammonium sulfate to 20 and 50% saturation, respectively. Following recovery of the insoluble fraction by centrifugation at 10000*g* for 10 min, this pellet was resuspended in a minimum of column buffer consisting of 50 mM Hepes, pH 7.5, 1 mM EDTA, and 0.1 mM dithiothreitol and applied to a Superdex S200 (Pharmacia) gel exclusion resin (2.6 × 114 cm) equilibrated with 50 mM NaCl in column buffer. Eluant fractions were screened by both sodium dodecyl sulfate−polyacrylamide gel electrophoresis (SDS−PAGE) and enzymatic assay for the presence of VanHst. Active fractions were pooled and applied to a MonoQ column (0.5 × 6.0 cm, Pharmacia) equilibrated in column buffer. Proteins were eluted with a linear gradient from 100 to 400 mM NaCl in column buffer over 50 column volumes. VanHst-containing fractions were pooled, and ammonium sulfate was added to a final concentration of 1.0 M. This sample was applied to a Phenyl Superose column (0.5 × 6.5 cm, Pharmacia) equilibrated with 1.0 M ammonium sulfate in column buffer. Proteins were eluted with a linear gradient from 1.0 to 0 M ammonium sulfate in column buffer over 50 column volumes. VanHst-containing fractions were pooled, desalted and concentrated with Millipore concentrators to 0.5 mg/mL. VanHst site mutants were purified in an identical fashion. In all cases, SDS−PAGE revealed a single Coomassie blue stained band migrating with an apparent mass of 36 kDa.

Assays. Protein concentration was determined by Bradford assay (*10*) using a Bio-Rad kit. Sample purity was determined by SDS−PAGE. During purification, VanHst enzyme activity was assayed by monitoring the decrease of NADH concentration in 1 mL reactions containing 100 mM sodium phosphate, pH 5.6, 100 μM NADH, and 10 mM pyruvate at 37 °C. NADH was detected by measuring absorbance at 340 nm, at which it's molar extinction coefficient is 6220 M^{-1} cm^{-1}. Kinetic assays of VanHst contained 100 mM sodium phosphate buffer, pH 5.6, saturating quantities of the nonvaried substrate, and 27.7 pmol of enzyme, unless otherwise specified. No background oxidation of NADH was observed (detection limit 0.001 absorbance units/min at 340 nm).

Data were analyzed by nonlinear least-squares methods using Grafit 3.0 (*11*). Kinetic parameters for purified VanHst were determined by fitting to eq 1. Inhibition experiments were analyzed by fitting to eqs 2, 3, or 4 for competitive, noncompetitive-mixed, or uncompetitive inhibition, respectively. Parameters obtained from the best fit are reported with standard errors to the fit.

$$v = V_{max}S/(K_m + S) \quad (1)$$

$$v = V_{max}S/[K_m(1 + I/K_{is}) + S] \quad (2)$$

$$v = V_{max}S/[K_m + S(1 + I/K_{ii})] \quad (3)$$

$$v = V_{max}S/[K_m(1 + I/K_{is}) + S(1 + I/K_{ii})] \quad (4)$$

Replots of slope and/or intercept of double reciprocal plots were linear.

The dependence of kinetic parameters on pH was performed in the following buffers each at 100 mM: sodium acetate, pH 4.0−5.5; sodium citrate, pH 5.5−7.0; Hepes, pH 7.0−8.5; and TAPS, pH 8.5−9.5. Data were fit to eq 5 as indicated above:

$$Y = \lim/(1 + [H^+]/K_1 + K_2/[H^+]) \quad (5)$$

where Y is the varied parameter (k_{cat}/K_m), lim is the limiting value of the kinetic parameter, $[H^+]$ is the hydrogen ion

Table 1: Purification of VanHst from *E. coli* BL21(DE3)/pETVanHst

sample	protein (mg)	activity (nmol/s)	specific activity (nmol/s/mg)	recovery (%)	purification (*n*-fold)
clarified lysate	139	19.3	60.5	100	
ammonium sulfate (20−50% saturation)	215	12.1	56.4	63	0.9
Sephacryl S200	27	8.45	313	44	5.2
Mono Q	10.9	3.23	296	17	4.9
Phenyl Superose	3.1	2.50	806	13	13.3

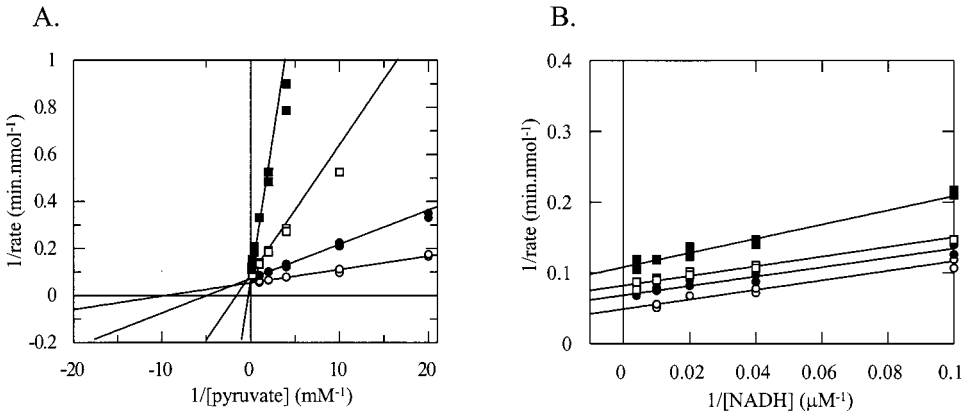

FIGURE 1: Inhibition of VanHst by oxamate. (A) Double reciprocal plot of the effect of increasing oxamate concentrations on the steady-state rate with varying pyruvate. Oxamate concentrations were 0 mM (○), 0.1 mM (●), 0.5 mM (□), and 2.5 mM (■). (B) Double reciprocal plot of the effect of increasing oxamate concentrations on the steady-state rate with varying NADH. Oxamate concentrations were 0 mM (○), 0.1 mM (●), 0.2 mM (□), and 0.4 mM (■).

concentration, and K_1 and K_2 are the ionization constants of the titrated groups.

The stereochemistry of the VanHst reaction product was determined as follows. VanHst reaction (1 mL) contained 25 mM pyruvate, 25 mM NADH, either 0 or 8 μg of VanHst in 100 mM Hepes, pH 7.0, and was incubated 16 h at room temperature. Reactions were passed through a 0.45 μM filter and used as substrates for the D-Ala-D-Lac ligase DdlN (*6*). Reactions (50 μL final volume) contained 10 mM $MgCl_2$, 10 mM KCl, 5 mM ATP, 5 mM D-alanine, 20 μg DdlN, and 25 μL of VanHst reaction products in Hepes, pH 7.0, and were incubated for 5 min at 37 °C. DdlN was purified and assayed by phosphate release activity as previously described (*6*).

Site-Directed Mutagenesis. Point mutations were introduced into *vanHst* using Stratagene's Quickchange mutagenesis kit. Thermocycled reactions were performed as described by the manufacturer's protocol with the exception that dimethyl sulfoxide was added to 5.0% (v/v). The primers used to construct Arg237Gln were 5′-GGTCATCAACAC-CGGACAGGGTGGGCTCATCG-3′ and 5′-CGATGAGC-CCACCCTGTCCGGTGTTGATGACC-3′. The primers used to construct Glu266Ala were 5′-CGTCGAAGGCGCG-GAGGGCATCTTCTACG-3′ and 5′-CGTAGAAGATGC-CCTCCGCGCCTTCGACG-3′. The primers used to construct His298Ala were 5′-GCGCATCACTCCGGCCACC-GCCTACTACACG-3′ and 5′-CGTGTAGTAGGCGGTG-GCCGGAGTGATGAGC-3′. Construction of each mutant was confirmed by complete sequencing of the gene.

RESULTS AND DISCUSSION

Overexpression and Purification of VanHst. The *vanHst* gene was amplified using Vent polymerase PCR from a clone obtained from a library of *S. toyocaensis* NRRL 15009 genomic DNA, which we had constructed previously (*3*). The amplified gene was cloned downstream of the T7 promoter in the expression vector pET22b, placing it under control of the bacteriophage T7 polymerase. Induction of mid-log cultures of *E. coli* BL21(DE3) for 3 h at 37 °C with isopropyl β-D-thiogalactopyranoside resulted in good expression of VanHst in a soluble form, as determined by SDS−PAGE analysis. Table 1 summarizes the four-step protocol developed to purify VanHst from soluble protein extracts of *E. coli*, yielding 3.1 mg of pure enzyme (Figure 1) from 2.5 g of cells. While VanHst could be detected in fractions by assaying for pyruvate-coupled NADH oxidation, endogenous *E. coli* D-LDHs were frequently contaminating during chromatographic separation and SDS−PAGE was required to identify VanHst enriched fractions. Contaminating D-LDHs were removed by the Mono Q column and are responsible for the apparent poor recovery and purification at this step.

Characterization of Steady-State Kinetic Parameters. Table 2 compares the steady-state kinetic parameters of purified VanHst with that of the enterococcal enzyme VanH (*12*). VanHst has nearly 17-fold lower K_m for pyruvate (K_m = 0.09 mM) than does VanH. This increase in apparent affinity is not paralleled in a decrease in catalytic rate, as VanHst's turnover number of 12 s^{-1} is only 3.3-fold less than that of VanH. VanHst has an overall efficiency of 1.3 × 10^5 M^{-1} s^{-1}, nearly an order of magnitude better than the value of 2.7 × 10^4 M^{-1} s^{-1} calculated for VanH. VanHst was also evaluated for its ability to reduce alternative substrates structurally similar to pyruvate. None of the substrates tested were preferred by VanHst over pyruvate with respect to K_m nor catalytic turnover. Compared to VanH, VanHst had lower K_m values for α-ketobutyrate and α-ketocaproate; however, these reductions were matched by near

Table 2: Characterization of Steady State Parameters of VanHst

	S. toyocaensis VanHst			*E. faecium* VanH[a]		
substrate	k_{cat} (s^{-1})	K_m (mM)	k_{cat}/K_m ($M^{-1}\,s^{-1}$)	k_{cat} (s^{-1})	K_m (mM)	k_{cat}/K_m ($M^{-1}\,s^{-1}$)
pyruvate	12 ± 0.3	0.09 ± 0.01	1.3×10^5	40	1.5	2.7×10^4
α-ketobutyrate[b]	5.7 ± 0.2	0.71 ± 0.1	8.0×10^3	35	2.6	1.3×10^4
α-ketocaproate[b]	1.4 ± 0.1	2.9 ± 0.5	4.8×10^2	2.4	20	1.2×10^2
α-ketoisocaproate		>100		5.2	31	1.7×10^2
α-ketoisovalerate		>100		5.2	150	3.5×10^1
phenylpyruvate		>100		<2		
NADH	13 ± 0.3	0.010 ± 0.001	1.3×10^6		0.021	
NADPH	16 ± 0.8	0.011 ± 0.001	1.5×10^6		0.002	

[a] Data from ref *12*. [b] Stereochemistry of reduction has not been independently determined but is assumed to be D specific.

Table 3: Product Inhibition Patterns for VanHst[a]

	NADH varied				Pyruvate varied	
	unsaturated with pyruvate		saturated with pyruvate		unsaturated with NADH	
product inhibitor	pattern	K_i (mM)	pattern	K_i (mM)	pattern	K_i (mM)
D-lactate	NC	$K_{ii} = 8.8 \pm 1.9$ $K_{is} = 7.4 \pm 0.1$	UC	$K_{ii} = 5.5 \pm 0.2$	NC	$K_{ii} = 3.9 \pm 0.3$ $K_{is} = 3.8 \pm 0.6$
NAD^+	C	$K_{is} = 2.1 \pm 0.1$	nd		NC	$K_{ii} = 3.3 \pm 0.8$ $K_{is} = 5.3 \pm 0.4$

[a] Abbreviations: NC, mixed-type noncompetitive inhibition; UC, uncompetitive inhibition; C, competitive inhibition; nd, not determined.

proportional decreases in k_{cat}, resulting in similar efficiencies of the two enzymes for these substrates. VanHst has no detectable α-ketoisocaproate and α-ketoisovalerate reductase activity at concentrations of these compounds nearing solution saturation. While not efficiently utilized, these compounds are reduced with measurable rates in the presence of VanH.

Table 2 also shows the lack of selectivity of VanHst in its choice of nicotinamide cofactor, using NADH and NADPH with equal efficiency. This contrasts with VanH from *E. faecium* which has a NADPH K_m of 2 μM, a full order of magnitude lower than that of NADH (*12*). This is also consistent with the observation that, unlike VanH (*12*), VanHst does not bind to 2′,5′-ADP agarose, a hallmark of many $NADP^+$-dependent enzymes (not shown).

Stereochemistry of the VanHst Reaction Product. The predicted D-specific stereochemistry of the VanHst reaction product was confirmed by utilizing the stereospecific incorporation of D-lactate into the depsipeptide D-alanine-D-lactate by the DdlN ligase of *A. orientalis* C329.2. DdlN was observed to release inorganic phosphate from ATP at a rate of 0.08 nmole/s when reaction products from VanHst were added. No rate was observed when the substrates of the VanHst reaction or when L-lactate was added at concentrations greater than those of the VanHst reaction products.

Inhibition of VanHst by Oxamate. Oxamate (**1**) is a pyruvate isostere and is known to be a competitive inhibitor of D-LDHs (*13*).

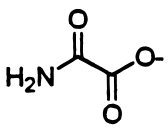

1

Oxamate is also a competitive inhibitor of pyruvate for VanHst with K_{is} of 28 ± 3 μM, 3.2-fold lower than the K_m for pyruvate (90 μM). This is in contrast to the relationship of these two parameters in the D-LDH of *L. plantarum*, in which the K_i (5 mM) for oxamate is a full order of magnitude larger than the pyruvate K_m (0.5 mM) (*13*). We also determined the effect of oxamate on VanHst NADH oxidation. The double reciprocal plot gave rise to parallel lines characteristic of uncompetitive inhibition with K_{ii} of 0.36 ± 30.57 mM (Figure 1). This is consistent with exclusive affinity for oxamate to the NADH·VanHst binary complex and is suggestive of an ordered BiBi kinetic mechanism.

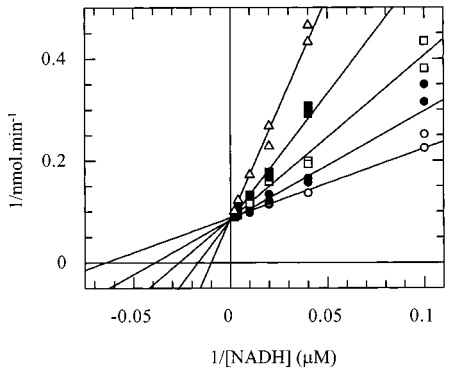

FIGURE 2: Inhibition of VanHst by NAD^+. Double reciprocal plot of the effect of increasing NAD^+ concentrations on the steady-state rate with varying NADH. NAD^+ concentrations were 0 mM (○), 1.0 mM (●), 2.5 mM (□), 5.0 mM (■), and 10 mM (△).

Product Inhibition Studies on VanHst. The kinetic mechanism of VanHst was further elaborated using the reaction products D-lactate and NAD^+ as inhibitors of the reduction of pyruvate. The inhibition patterns observed when VanHst activity was assayed in the presence of products are summarized in Table 3. NAD^+ was a competitive inhibitor of NADH, indicating that both these molecules bind the same enzyme form (Figure 2). No other competitive inhibition patterns were observed. Both NAD and D-lactate were mixed-type noncompetitive inhibitors of pyruvate at subsaturating concentrations of the nonvaried substrate. D-lactate also served as a mixed-type inhibitor of NADH oxidation. However, this inhibition pattern converts to uncompetitive

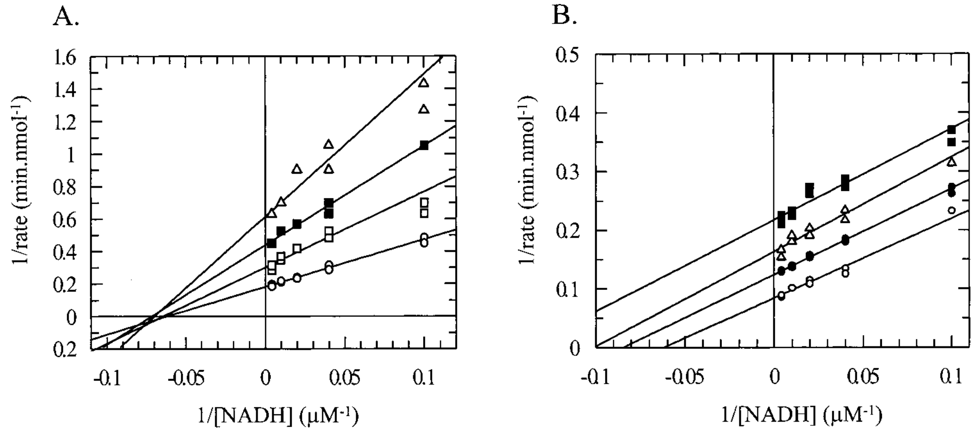

FIGURE 3: D-Lactate inhibition patterns for VanHst. (A) Double reciprocal plot of the effect of increasing D-lactate concentrations on the steady-state conversion of NADH at 0.05 mM pyruvate. D-Lactate concentrations were 0 mM (○), 0.1 mM (●), 5.0 mM (□), 10 mM (■), and 20 mM (△). (B) Double reciprocal plot of the effect of increasing D-lactate concentrations on the steady-state conversion of NADH at 0.2 mM pyruvate. D-Lactate concentrations were 0 mM (○), 0.1 mM (●), 5.0 mM (□), 10 mM (■), and 20 mM (△).

Scheme 1

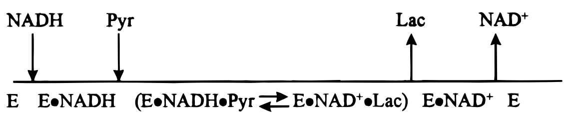

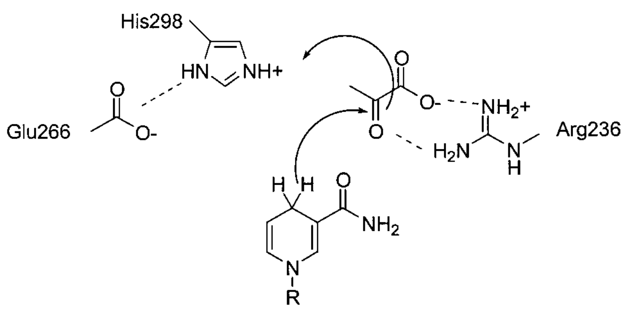

FIGURE 4: Predicted molecular mechanism of D-LDHs. Numbering of residues is based upon the VanHst sequence.

as pyruvate concentration is increased to saturating levels (Figure 3). These patterns of inhibition are consistent with VanHst utilizing an ordered BiBi kinetic reaction mechanism where NADH binds first and pyruvate binds second. After hydride transfer occurs in the ternary complex, product release is also ordered with lactate leaving first followed by NAD^+ (Scheme 1).

Site-Directed Mutagenesis of VanHst. Mutagenesis studies conducted with the D-LDH's of *Lactobacillus plantarum* and *Lactobacillus bulgaricus* have identified key amino acids involved in substrate binding and catalysis (*13*−*15*). These results have suggested a mechanism of hydride transfer (Figure 4) where a conserved Arg interacts with both the keto and carboxylate groups of pyruvate, positioning the substrate and polarizing the α-keto group. An invariant His acts as a catalytic base, and a conserved Glu interacts with the protonated His. The recently determined 3D-structure of the D-LDH of *L. plantarum* has confirmed the presence of the residues Arg235, Glu264, and His296, which were predicted to be important by mutagenesis, in the active-site region (*9*).

Alignment of the amino acid sequence of VanHst with these and other D-LDH's indicated that residues Arg237, Glu266, and His298 of VanHst may be similarly important in enzyme function (Figure 5), a hypothesis which we

S. toyocaensis	T G	R_{237}	G G	E G	E_{266}	E G	.... T P	H_{298}	T A
E. faecium	T G	R_{231}	G P	E G	E_{260}	E E	.... T P	H_{292}	T A
Synechocystis	T S	R_{235}	G H	E E	E_{264}	E E	.... T A	H_{296}	Q G
L. plantarum	F A	R_{235}	G T	E Y	E_{264}	T K	.... T P	H_{296}	T A

FIGURE 5: Primary sequence alignment of various D-lactate dehydrogenases. Alignment calculated by the CLUSTAL W method (17). The conserved residues mutated in this study are boxed.

explored by site-directed mutagenesis. Each of the VanHst mutants, Arg237Gln, Glu266Ala, and His298Ala, were expressed in *E. coli* BL21(DE3) and purified to homogeneity and their steady-state parameters determined (Table 4).

Arg237Gln had essentially wild-type K_m for NADH, but had a 30-fold reduction in k_{cat} and a nearly 60-fold increase in pyruvate K_m, reflecting a decreased capacity in both catalytic rate and in α-ketoacid substrate binding. This 1780-fold decrease in k_{cat}/K_m is comparable in direction, but not magnitude, to that found in the Arg235Gln mutant of *L. plantarum* D-LDH which resulted in a 1.5×10^5-fold decrease in k_{cat}/K_m (*13*). Nevertheless, these results are consistent with a role in substrate binding and catalysis for VanHst Arg237 as predicted by the mechanism in Figure 4.

The His298Ala mutant showed a 10^4 fold drop in k_{cat}/K_m, primarily as a result of a 600-fold reduction in k_{cat} to 0.02 s^{-1}, while pyruvate K_m increased 16-fold. The poor activity precluded accurate measurement of the NADH dependence. This is comparable to the magnitude of k_{cat}/K_m decrease in the His296Tyr mutant in the *L. plantarum* D-LDH, though in this case, there is negligible effect on K_m (1.4-fold drop) (*15*). Thus, His298 of VanHst plays and important function in catalysis consistent with a role as an active site acid which provides a proton to the product hydroxyl (Figure 4).

The Glu266 equivalent in the *L. plantarum* D-LDH crystal structure (Glu264) is positioned within hydrogen-bonding distance of the catalytic His (*9*). In VanHst, a Glu266Ala mutation has only a modest effect on k_{cat} (1.5-fold decrease at pH 5.6); however, K_m for pyruvate was increased 10-fold (Table 4). The NADH K_m was relatively unchanged. The corresponding Glu264Gly mutation in *L. bulgaricus* (*14*) and Glu264Gln mutation in *L. plantarum* (*16*) D-LDHs have been prepared, and these show, respectively, 62 and 1740-fold decreases in k_{cat}/K_m for pyruvate. The Glu264Asp mutation

Table 4: Characterization of Steady-State Parameters of VanHst Mutants

	pyruvate			NADH		
VanHst	k_{cat} (s^{-1})	K_m (mM)	k_{cat}/K_m (M^{-1} s^{-1})	k_{cat} (s^{-1})	K_m (μM)	k_{cat}/K_m (M^{-1} s^{-1})
WT	12 ± 0.3	0.094 ± 0.01	1.3×10^5	13 ± 0.3	10 ± 1	1.3×10^6
Arg237Gln	0.40 ± 0.01	5.5 ± 0.2	7.3×10^1	0.4 ± 0.02	7.2 ± 0.9	5.6×10^4
Glu266Ala	8.3 ± 0.2	2.6 ± 0.1	2.3×10^4	9.5 ± 0.2	8.3 ± 0.7	1.1×10^6
His298Ala	0.02 ± 0.001	1.5 ± 0.4	1.3×10^1	ND	ND	

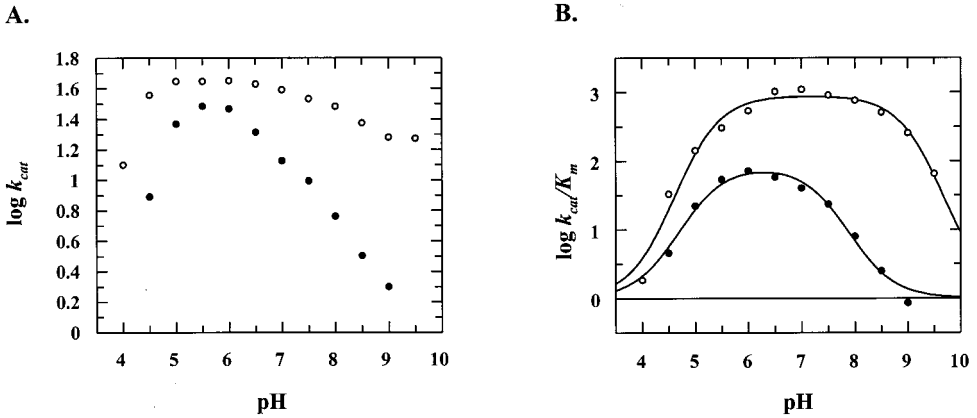

FIGURE 6: Comparison of the pH dependence of the steady-state rate pyruvate conversion parameters of VanHst wild-type and Glu266Ala mutant. Effect of pH on the enzyme turnover number, k_{cat} (A) and specificity, k_{cat}/K_m (B). Key: wild-type (○), Glu266Ala (●).

in *L. plantarum* has also been prepared and shows a 40-fold decrease in pyruvate k_{cat}/K_m (*16*). Further analysis of the pH dependence of *L. bulgaricus* Glu254Gly mutant revealed a 2 pH unit shift toward acidic pH in a single k_{cat}-dependent pK_a (*14*). This observation was attributed to Glu264 modulation of the ionization of the catalytic His, a hypothesis which is consistent with the proximity of these residues in the *L. plantarum* D-LDH crystal structure (*9*). However, in the *L. plantarum* Glu264Gln and Glu264Asp mutants, there was generally little change in the pH dependence of kinetic parameters, though their magnitudes were significantly decreased as indicated above (*16*).

Wild-type VanHst shows a complex k_{cat} dependence on pH with both acidic and basic pK_as (Figure 6). However, the data in toto do not fit a bell-shaped pH dependence curve, and it would appear that the loss of activity on the acidic arm of the curve (pH <5) may be a result of several equilibria. However, the k_{cat}/K_m dependence on pH could readily be fit to bell shaped curves. The acidic pK_a for both the wild-type and Glu226Ala enzymes remained unchanged at 4.7 ± 0.1, while the basic pK_a was lowered by almost 2 pH units 9.7 ± 0.1 to 7.9 ± 0.1. These results are consistent with an important role for Glu266 in the productive interaction of pyruvate with the VanHst·NADH complex and to catalysis. The positioning of the His-Glu pair in the *L. plantarum* D-LDH structure demonstrates a close interaction between these residues and our pH dependence results are consistent with a similar arrangement in VanHst. These results also imply that Glu266 helps to maintain His264 in a protonated state through a broad range of pHs. This information is therefore exploitable in drug design for VanH from enterococci.

CONCLUSIONS

VanH is one of three enzymes absolutely required for high level glycopeptide resistance in VRE and antibiotic producing organisms. These studies using the VanHst enzyme from an glycopeptide antibiotic producing organism provide the appropriate foundation for exploitation of VanH as a drug target and furthermore demonstrate the value in studying resistance mechanisms in streptomycetes. This analysis of the mechanism of VanHst indicates that compounds which share structural similarity between both substrates and which could take advantage of interactions with active-site Arg and His protonated side chains have the potential to act as potent VanH inhibitors and could serve as the starting point for compounds which rescue vancomycin activity in VRE.

REFERENCES

1. Arthur, M., and Courvalin, P. (1993) *Antimicrob. Agents Chemother. 37*, 1563−1571.
2. Walsh, C. T., Fisher, S. L., Park, I.-S., Prahalad, M., and Wu, Z. (1996) *Chem. Biol. 3*, 21−28.
3. Marshall, C. G., Lessard, I. A. D., Park, I.-S., and Wright, G. D. (1998) *Antimicrob. Agents Chemother. 42*, 2215−2220.
4. Marshall, G. C., Broadhead, G., Leskiw, B., and Wright, G. D. (1997) *Proc. Natl. Acad. Sci. U.S.A. 94*, 6480−6483.
5. Marshall, C. G., and Wright, G. D. (1997) *FEMS Microbiol. Lett. 157*, 295−299.
6. Marshall, C. G., and Wright, G. D. (1998) *J. Bacteriol. 180*, 5792−5795.
7. Lessard, I. A., Pratt, S. D., McCafferty, D. G., Bussiere, D. E., Hutchins, C., Wanner, B. L., Katz, L., and Walsh, C. T. (1998) *Chem. Biol. 5*, 489−504.
8. Arthur, M., Molinas, C., Dutka-Malen, S., and Courvalin, P. (1991) *Gene 103*, 133−134.
9. Stoll, V. S., Kimber, M. S., and Pai, E. F. (1996) *Structure 4*, 437−447.
10. Bradford, M. M. (1976) *Anal. Biochem. 34*, 248−254.
11. Leatherbarrow, R. J. (1992) *Grafit. Ver 3.0*, Erithacus Software Ltd., Staines, U.K.
12. Bugg, T. D. H., Wright, G. D., Dutka-Malen, S., Arthur, M., Courvalin, P., and Walsh, C. T. (1991) *Biochemistry 30*, 10408−10415.
13. Taguchi, H., and Ohta, T. (1994) *J. Biochem. 115*, 930−936.

14. Kochhar, S., Chuard, N., and Hottinger, H. (1992) *J. Biol. Chem. 267*, 2098−20301.
15. Taguchi, H., and Ohta, T. (1993) *J. Biol. Chem. 268*, 18030−18034.
16. Taguchi, H., Ohta, T., and Matsuzawa, H. (1997) *J. Biochem. (Tokyo) 122*, 802−809.
17. Thompson, J. D., Higgins, D. G., and Gibson, T. J. (1994) *Nucleic Acids Res. 22*, 4673−4680.

BI982843X